Faraday Rotation of the CaO *F* Band and 3557 Å Zero-Phonon Peak*

JAMES C. KEMP, WILLIAM M. ZINIKER, JAMES A. GLAZE, AND JACK C. CHENG
Department of Physics, University of Oregon, Eugene, Oregon 97403
(Received 8 January 1968)

The absorption band centered at 3.65 eV (3350 Å) seen in both neutron-irradiated and Ca-excess CaO crystals has been assigned to the *F* center. A sharp peak is seen adjacent to this band at 3557 Å, and has long been conjectured to be the zero-phonon line of the *F* center. Evidence is given here that supports this identification. Faraday-rotation experiments have been carried out on both the *F* band and the 3557 Å line, including studies using the method of ESR-sensitive Faraday rotation, which directly identifies rotation peaks due to paramagnetic centers. Such studies were earlier reported only on the 3.65-eV band, with low spectral resolution; in the new data, the spectral rotation of the sharp peak is revealed, and a more accurate pattern for the band is given. The magneto-optic behavior of the sharp peak is found to be similar to that of the band; both are paramagnetic and react in the same way to saturation of the *F*-center ESR line. A model featuring large Jahn-Teller distortion ϵ of the *F*-center p state predicts a dispersionlike rotation for the zero-phonon peak, with amplitude of order $(\lambda/\epsilon)\tanh(\mu H/kT)$ times the amplitude of the dispersion associated with the absorption peak. The measured pattern has this shape, and agrees in sign and amplitude with the model if we take $\lambda=-7\times10^{-3}$ eV, from the second moment of the circular dichroism of the *F* band; and $\epsilon\simeq0.12$ eV $\simeq1000$ cm^{-1}, comparable with the distance between the zero-phonon and band peaks ($\simeq0.16$ eV). Though our magneto-optical pattern is thus explainable in terms of a quenched-orbital-momentum model, certain other considerations suggest that quenching is small or marginal, the Jahn-Teller well depth $\frac{1}{4}\epsilon\sim250$ cm^{-1} being of the order of the mean vibrational quantum. Presumably the Faraday rotation of the zero-phonon peak is a mixture of dispersionlike and dispersion-derivativelike terms of comparable magnitudes, but the second is suppressed under our experimental conditions.

I. BACKGROUND

THE *F* center, a high-symmetry one-electron system, is an ideal structure in which to discuss the electron-lattice coupling in point defects in solids. For example, this system affords an opportunity to analyze in some detail the coupling to local modes arising from the lattice distortion, since fairly simple electronic wave functions can be used, and prominent local modes can be easily discerned. Unfortunately, in alkali-halide *F* centers the coupling parameter S (Huang-Rhys factor) is so large that zero-phonon and resolved multiphonon peaks are of vanishing amplitude, and the only information comes from the shape and temperature dependence of the *F* band, which reflect only integrated effects of the vibrational spectrum. In the divalent lattices of the simple oxides MgO, CaO, SrO, and BaO, the *F* electron is much more strongly localized than in alkali halides, certainly in MgO,[1] and the electron-lattice coupling picture ought to be much different. For one thing, the equilibrium lattice distortion appears to be greater.[2] Secondly, if the *F* electron is strongly localized inside the nearest cation shell in the p state as well as in the ground state, we might expect a smaller S on the ground that the Stokes shift ΔE depends on the difference in effective charge inside the vacancy between initial and final states. This is not a very convincing speculation. However, it seems to be supported by exploratory calculations by Bennett,[3] who finds S as low as 4 or 5 for CaO, for example; this, of course, depended on the effective vibrational frequency ω_D used, since $S=\Delta E/(2\hbar\omega_D)$. The integrated zero-phonon peak intensity at 0°K being $\exp(-S)$, relative to the integrated band intensity,[4] the zero-phonon peak would in that case be visible.

The strong absorption band at 3.65 eV, half-width about 0.25 eV seen in both neutron-irradiated and additively colored (Ca-excess) CaO, is presently accepted as the *F* band by virtue of correlation of the band intensity with the *F*-center ESR line intensity,[5] and as a result of certain magneto-optical experiments reported earlier[6] and refined in the present work.

A sharp zero phononlike peak is seen on the low-energy side of the CaO *F* band, at 3557 Å, visible at 77°K and below. Some weaker sharp peaks are also detectable between 3557 and 3350 Å (band maximum), suggestive of multiphonon structure. We had wondered for some time whether the 3557 Å peak was indeed the *F*-center zero-phonon line, as the appearance surely suggests. The answer to this question could have been sought by conventional means, such as by correlating the peak intensity with that of the band for a sequence of samples, followed by an attempt to fit the intervals between the 3557 Å and lesser peaks to critical transition frequencies in the CaO phonon spectrum, and so on. The CaO phonon spectrum actually is not available. Aside from that, it is well known that individual absorption spectra are hard to isolate in the alkaline earth oxides, usually many point-defect species being present.

* Supported by AFOSR (Solid-State Sciences Division).
[1] J. C. Kemp and V. I. Neeley, Phys. Rev. **132**, 215 (1963).
[2] W. P. Unruh and J. W. Culvahouse, Phys. Rev. **154**, 861 (1967).
[3] H. S. Bennett (unpublished calculations); Bull. Am. Phys. Soc. **13**, 420 (1968).
[4] See, for example, D. B. Fitchen, R. G. Silsbee, T. A. Fulton, and E. L. Wolf, Phys. Rev. Letters **11**, 275 (1963).
[5] D. H. Tanimoto, Ph.D. thesis, University of Oregon, Eugene, Oregon, 1966 (unpublished).
[6] J. C. Kemp, W. M. Ziniker, and J. A. Glaze, Proc. Brit. Cer. Soc. **9**, 109 (1967); also see a paper on the MgO *F* band, J. C. Kemp, W. M. Ziniker, and J. A. Glaze, Phys. Letters **22**, 37 (1966).

Evidence is given here that the 3557 Å line is the F-center zero-phonon line, based on magneto-optic experiments. We also present a refined curve of the Faraday-rotation pattern of the F band with a recalculation of the spin-orbit parameter.

II. EXPERIMENTAL METHOD

The present experiments pertain to the optical Faraday rotation at helium temperatures associated with the 3.65-eV absorption band and 3557 Å line in neutron-irradiated CaO crystals. This is an extension of earlier work, in which various rotation patterns due to point defects in MgO and CaO were reported.[6] Faraday rotation analogous to that seen in alkali-halide F centers was seen in the MgO F band as well as in CaO.

The apparatus and techniques used for this work are described briefly as follows[6,7]: (a) The Faraday rotation is recorded, normally at either 4.2°K or at approximately 1.8°K, using a superconducting magnet with maximum field about 50kG. (b) A magneto-optical double-resonance method is used, in which changes in the Faraday rotation are detected upon saturation or inversion of electron spin resonance in the sample; this is referred to as FR-ESR or microwave-sensitive Faraday rotation.

The FR-ESR method directly connects an absorption-band rotation pattern of a paramagnetic species with the ESR line or lines of the species, being thus a qualitative analytical tool. The connection is completely specific only if the ESR excitation is resolved, and if certain cross-relaxation and thermal effects are not of consequence. Even without such conditions, the method can demonstrate that the species causing an absorption band is paramagnetic when definite signals are gotten. It also serves to extract the rotation of a given species, or strictly speaking the paramagnetic part of this rotation, from interfering rotations such as crystal interband and spurious apparatus rotations.

The output data of an FR-ESR experiment furnish a curve $\theta_{\text{para}}(\lambda)$ of the species excited by ESR, as in Figs. 1 and 4 of this paper. Data are obtained by either of two procedures: (1) By scanning in λ through a spectral region, first with microwaves off, thence with an ESR resonance saturated, and taking the difference in scans of the Faraday rotation; or (2) by switching the microwave line off and on, at discrete wavelengths λ_i, and noting the rotation changes $\Delta\theta(\lambda_i)$. Procedure (1) is convenient for narrow rotation patterns (zero-phonon lines); but we prefer (2) for broad patterns (e.g., of the F band), due to stability problems with wide sweeps.

Sources of error in our measurements were not well understood in the preliminary stages,[6,7] but are now fairly well controlled. It is to be remembered that measurements of this kind are difficult in the uv, and that the CaO samples used have high absorbance in the F band, in order to override the impurity bands, and are optically imperfect. For FR-ESR the sample is rather delicately positioned inside a Ka-band (35-GHz) cavity, with 2-mm-diam light ports; the cavity is held inside the superconducting solenoid. A sensitive optical alignment is required. The main errors in measuring rotation are related to the following:

(a) Resolution. The smallest monochromator slit width consistent with useable signal-to-noise ratio, determined by the net transmitted light, is used. With finite resolution, the detected rotation pattern can be distorted in a complicated way, particularly where absorbance varies rapidly; e.g., the zeros of the pattern can be shifted (note Fig. 1).

(b) Degeneration, i.e., spurious reduction, of the detected rotation. In the spinning analyzer system,[6,7] the rotation angle is detected as the phase of the sinusoidal photomultiplier voltage. The latter is the vector (phasor) sum of the true signal, i.e., that from light at the measuring wavelength plus any *coherent* but spurious signal. Rotation of the total-signal phasor, due to an incremental rotation of the true-signal phasor, is less than the true-signal rotation by a factor of the order $|V_t|/(|V_t|+|V_s|)$, where V_t and V_s are the amplitudes of the true and spurious signals, respectively. The chief degeneration comes from stary light arising originally in the monochromator or as sample fluorescence; if polarized (even partially), such light passes through the spinning analyzer along with the true light giving a spurious coherent signal. The effect is clearly greatest in spectral regions where the net transmitted light and the analyzer-polarizing efficiency are low, and where beam depolarization from scattering, etc., is great; it increases generally toward shorter wavelengths. Since our earlier papers, we have looked into this problem carefully, and have measured the amount of stray-light degeneration by inserting a second monochromator in the detection end of the system, which virtually eliminates stray light and allows accurate comparisons to be made. In the present work, covering the CaO F-band spectral region, adequate stray-light reduction was had by using a uv-passing filter (Corning 7-54) over the photomultiplier; this filter is opaque for $\lambda \gtrsim 3700$ Å, where most of the stray light was found.

It was important to realize that simple random deterioration of the beam polarization, e.g., by scattering at poorly polished sample faces, as well as inefficiency of the analyzer or other components, do not themselves affect the detected polarization angle or measured rotations. But the "true signal" is reduced by such losses, leading to degeneration if the true signal amplitude falls below that of spurious signals.

Apart from the usual background Faraday rotation[6] (crystal interband rotation, etc.), there is an appreciable zero-field ($H=0$) effect in our rotation curves, as revealed in trace C of Fig. 3. In the FR-ESR procedure,

[7] W. M. Ziniker, Ph.D. thesis, University of Oregon, Eugene, Oregon, 1967 (unpublished).

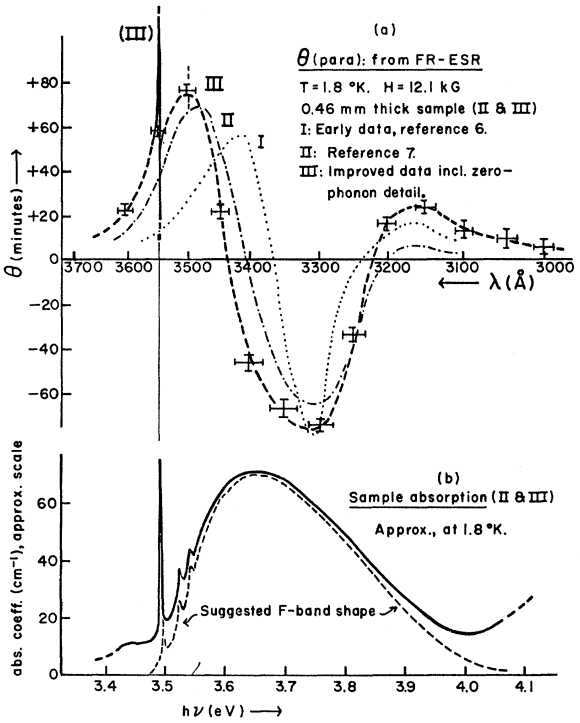

FIG. 1. Paramagnetic Faraday rotation (a) of the CaO F band and 3557 Å zero-phonon line, as determined from magneto-optical double resonance of the F-center ESR line. Curves I, II, and III are plotted from discrete-λ measurements, made by observing the rotation changes $\Delta\theta(\lambda_i)$ caused by saturating or pulse-inverting the ESR line with 35-MHz microwave power; except that rotation around the zero-phonon line was determined by a high-resolution continuous scan (Figs. 3 and 4) and superimposed on III. The sample absorption is shown in (b).

both zero-field and background rotations are automatically eliminated by subtraction. The zero-field effect, however, is a little mysterious and deserves comment. It has two parts; first, an inconsequential part arising in the apparatus and varying slowly with λ. But there is a second component which peaks up on the sample absorption peaks, with spectral shape at least approximately following the dispersion patterns of the absorption peaks. This is again rather definitely a spurious effect and does not indicate any significant property such as rotatory power in point-defect species causing the absorption peaks. A suggested cause is macroscopic strain-related birefringence in the sample, which like the refractive index would show peaks at all absorptive transitions; we can show, however, that this would not give a dispersionlike rotation. The more likely cause is simple rotation of the polarization as the beam passes through the sample faces, if these are not quite normal to the beam, or some very similar effect. Such rotation should be proportional to the dispersion and have periodicity π relative to orientation of the beam polarization (with given sample orientation), which is in fact observed. The effect can be "tuned out" by geometrical adjustments, but this was not usually convenient in our measurements. We determined that the net H-dependent rotation, i.e., $\theta(\lambda,H)-\theta(\lambda,0)$, was independent of $\theta(\lambda,0)$ and is correctly taken as the Faraday rotation.

III. RESULTS: PARAMAGNETIC ROTATION IN THE F-BAND REGION FROM FR-ESR

In Fig. 1 are displayed the absorption of neutron-irradiated CaO and corresponding paramagnetic rotation from FR-ESR double resonance, in the F-band region at 1.8°K with $H=12$ kG. The samples used were from crystals irradiated in the ORR reactor (Oak Ridge) to about $10^{18}nvt$ (12-h irradiation), and subsequently heat-bleached by trial and error until the F band was moderately well resolved from neighboring bands.[5] The absorption curve and the rotation curves II and III pertain to the same sample; rotation curve I pertains to a sample of slightly different F-center density.

The absorption curve in Fig. 1(b) was taken from an accurate spectrophotometer trace at 77°K, readjusted slightly to accord with single-beam transmittance measurements made in the Faraday rotation apparatus[6] at about 1.8°K.

The Faraday-rotation curves I, II, and III refer to changes $\Delta\theta$ effected by saturation, (in II and III) of the F-center ESR line; or by adiabatic rapid passage inversion[6] (giving an equivalent signal upon division by 2) in I. All three curves represent data points from $\Delta\theta$ values measured at discrete wavelengths (procedure 2 above), though data points and error bars are omitted in II and III. On curve III we have superimposed a high-resolution trace covering the 3557 Å region, to be discussed in detail later.

Apart from the sharp peak details, curve III is taken as the most accurate representation of θ_{para} of the F band. Curves I and II are from earlier experiments, I being from Ref. 6. The experimental discrepancies between these curves are largely a matter of varying spectral resolution and of λ-dependent degeneration of the detected rotation, as told in Sec. II. The qualitative shapes (ignoring the sharp-line detail) of all three curves are similar. Resolution was very poorly controlled in I and was, in fact, not measured, since the degree of distortion of the pattern (shift in the zeros and maxima) due to finite bandwidth was not at first reckoned with. The right-hand (short λ) positive peak in θ is apparently degenerated in II. In III we eliminated the stray-light and spurious-signal problem in this region and believe this curve to be reliable.

A. Relaxation Behavior

Some relaxation-time aspects of the FR-ESR signals are illustrated in Fig. 2. These observations were made to substantiate our identification of the FR-ESR patterns with the F center. No quantitative study of spin-lattice relaxation was intended. It is probable that somewhat complex extrinsic processes control the effective T_1

of the CaO F center (as in MgO[8]) in samples so far studied. That this is so seems to follow from the H dependence (T_1 appears to be less at 3 kG than at 11 kG[5,6]) and perhaps from the concentration dependence. Relaxation of θ_{para} (at $\lambda\sim3500$ Å) after rapid passage inversion of the F-center ESR line is shown in Fig. 2(b) for a sample before and after heat treatment. The treatment was such as reduce the F-center spin density slightly, by less than a factor 2, but to considerably reduce the intensities of nearby ESR lines.[6] The almost fourfold increase in the effective T_1 may be due to general strain reduction; or the annealing out of those F centers in badly strained regions or those near impurities, reducing cross-relaxation rates. Relaxation following simple ESR saturation looks quite similar to the traces in Fig. 2(b).

No evidence for severely nonexponential relaxation, such as from hot-phonon effects,[9] is seen in relaxation from the inverted state. Results of a critical experiment that we referred to previously[6] are illustrated in Fig. 2(a), showing the effect of successive rapid passage spin inversions on θ_{para} spaced at intervals short compared to the relaxation time. The lower, middle, and upper dashed levels correspond to spin temperatures T (thermal equilibrium), ∞, and $-T$, respectively. The alternate transitions from positive to negative temperatures and vice versa show very dramatically that neither a general heating up of the lattice, nor so-called hot-phonon effects, are taking place. The possibility that all paramagnetic species in the sample are heated up indirectly via ESR excitation of the F center, which would make the identification of the FR-ESR pattern of the F band highly uncertain, is clearly ruled out. Nevertheless, cross relaxation to other species by spin-spin interaction[10] is not eliminated. A logical picture is that the F centers are coupled to certain "fact" intrinsic relaxors, such as Fe^{2+}, with a slow cross-relaxation time T_{12}; this being the effective time constant observed [Fig. 2(b)]. The fast relaxors are scarcely heated up, thus any Faraday rotation attributed to them would not change and would not contribute to the FR-ESR signal. Alternatively, the intermediary spins might have slow intrinsic T_1, yet fast compared to the F-center T_1, and be coupled to the F centers with a very short T_{12}; the recorded FR-ESR relaxation time is then the T_1 of the intermediary species. This case seems doubtful on the general ground that one is unlikely to find a species other than the F center itself with an intrinsic T_1 as long as 25 sec or longer at $T\sim2$°K.

The remaining ambiguity in the FR-ESR identification of the F band is that the observed ESR excitation width, in Gauss is much larger than the intrinsic F-center ESR linewidth, which is <1 G. An interaction width of ~20 G was shown in earlier work,[6] wherein we

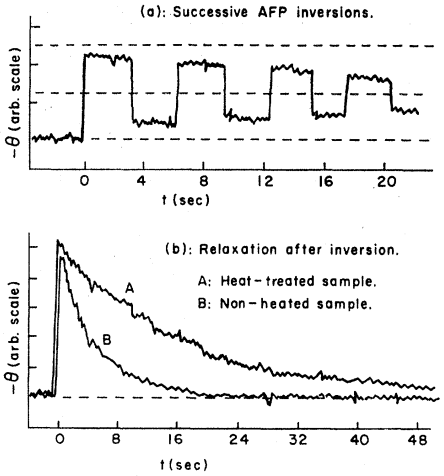

FIG. 2. Thermal relaxation of the CaO F-band paramagnetic Faraday rotation at 1.8°K, $H=12$ kG, following adiabatic rapid passage inversion of the ESR line by frequency sweep. The effective T_1 as seen in (b) is sample-dependent and is found to increase considerably upon heat-annealling the neutron-irradiated samples. A sequence of AFP inversions at intervals $<T_1$ in a heated sample (effective $T_1\sim30$ sec) is shown in (a), wherein one sees that successive transitions between positive and negative spin temperatures take place. The inversion time used was about 5 msec.

explained that an instrumental broadening, related to the long relaxation time, was the probable cause and is not easy to eliminate. As exemplified in the FR-ESR trace of the 3557 Å line, Fig. 3, we have not been able to reduce this width as yet. It might be argued that some small satellitelike lines near the F-center ESR line[11] are excited (directly, rather than by cross relaxation), and their optical transitions can contribute to the FR-ESR signal. But numerically, at least in heat-treated samples, the integrated intensity of such lesser lines is small compared to that of the F-center line; and a very crude but direct estimate of the rotation pattern amplitude, using only the F-center spin density and a theoretically reasonable spin-orbit parameter λ, appears to account for the experimental magnitude.[6] To attribute the rotation pattern to a species with, for example, a density less than one-tenth that of the F center would require a species with very large λ, at least of order 1000 cm^{-1} assuming an alkali atomlike structure, for the sake of argument.

B. Spin-Orbit Coupling Computation

We gave an earlier estimate of the p-state spin-orbit constant λ, based on the alkali atom model with rigid magnetic shift, with the F band assumed Gaussian.[6] A "blind" formula for the central $\theta(E)$ peak height was used, involving only the F-center density N, the oscillator strength f, and λ as essential unknowns. No data from the absorption band itself were needed, which was of some advantage since the CaO F band is incompletely

[8] J. S. Bennett, R. L. Hartman, and J. G. Castle, Bull. Am. Phys. Soc. **11**, 834 (1966).
[9] P. L. Scott and C. D. Jeffries, Phys. Rev. **127**, 32 (1962).
[10] P. R. Solomon, Phys. Rev. **152**, 452 (1966).
[11] J. E. Wertz, J. W. Orton, and P. Auzins, Discussions Faraday Soc. **31**, 140 (1961).

resolved. Using N as gotten from ESR data to fit the detected θ_{para} peak we concluded $(f\Delta)\cong-55$ cm^{-1} or $\Delta\cong-70$ cm^{-1} for $f=0.8$.

Formulas of Henry, Schnatterly, and Slichter[12] relate $\Delta=\frac{1}{2}3\lambda$ to moments of the magnetic circular dichroism. To use them one needs $A\equiv\int\alpha(E)dE$, where α is the ordinary absorption coefficient (i.e., for unpolarized light or for light of any polarization when $H=0$); and the mean energy $\bar{E}\equiv\int E\alpha(E)dE$. We define the circular dichroism as $\beta(E)\equiv\alpha_+(E)-\alpha_-(E)$, where $\alpha_\pm$ pertain to the two circular polarizations; this is *twice* the quantity $\alpha_+(E)-\alpha(E)$ appearing in the HSS equations. The HSS first moment can be written

$$\Delta E_+=(2A)^{-1}\int(E-\bar{E})\beta(E)dE=\tfrac{2}{3}\Delta\langle S_z\rangle. \qquad (1)$$

To compute $\beta(E)$ from the Faraday rotation one has by Kramers-Kronig inversion[13]

$$\beta(E)=\frac{4}{t}\frac{2E}{\pi}\int\frac{\theta(E')dE'}{(E')^2-E^2}\cong\frac{4}{\pi t}\int\frac{\theta(E')dE'}{E'-E}, \qquad (2)$$

wherein t is the sample thickness.

The F band at low temperatures in heat-treated samples is discernible enough so that A and $\bar{E}$ may be measured. From Fig. 1(b) we obtained A, with an apparent error of about $\pm10\%$, and found $\bar{E}=3.7$ eV. Using (2) with curve III of Fig. 1(a) we computed $\beta(E)$, which roughly resembles $\partial\alpha/\partial E$ (ignoring the zero-phonon detail), with amplitudes ±1.3 cm^{-1}. With $\langle S_z\rangle=\frac{1}{2}\tanh(\mu H/kT)=0.21$ at 1.8°K and $H=12$ kG, we obtained from Eq. (1),

$$\Delta=-(80\pm10)\text{ cm}^{-1},$$

thus

$$\lambda\cong-60\text{ cm}^{-1}\cong-0.7\times10^{-2}\text{ eV}. \qquad (3)$$

The estimated error here mostly has to do with evaluating the absorption integral A, in view of overlapping bands and baseline uncertainty in $\alpha(E)$. Being an integral-type calculation, in which errors in individual data points of $\theta(E)$ and $\alpha(E)$ are averaged out somewhat, and being based on the semirigorous theory of Ref. 12, this result should be reliable. That the crude earlier estimate[6] agrees so well must be accidental, but it tends to independently substantiate the finding that f is close to unity, as was found in correlating optical absorption and ESR intensities.[5]

[12] C. H. Henry, S. E. Schnatterly, and C. P. Slichter, Phys. Rev. **137**, A583 (1965).

[13] The approximation on the far right in Eq. (2) is very adequate for fractionally narrow bands, i.e., of width much less than the center frequency; it follows merely from $(E')^2-(E)^2\simeq2E(E-E')$ near E.

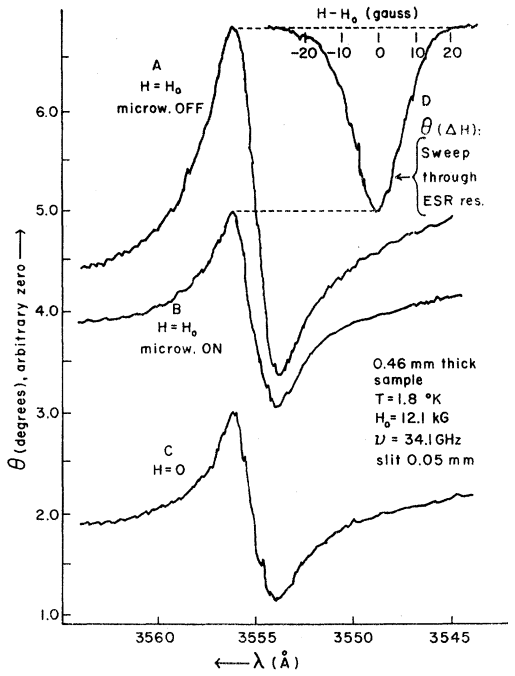

FIG. 3. FR-ESR double resonance of the 3557 Å zero-phonon line in CaO. A spurious zero-field optical rotation, dependent on apparatus adjustments, marks the location of the line in C, the $H=0$ trace. The Faraday rotation at 12 kG is the difference between curves A and C. Curve B is the net rotation seen while saturating microwave power is applied steadily to the F-center spin resonance. At upper right is the resonance curve, showing the transition from curves A to B and back (at a fixed λ) as H is swept through the ESR line ($g=2.000$).

IV. RESULTS: ROTATION AND FR-ESR CURVES OF 3557 Å LINE

In Fig. 3 are drawn slow-rotation traces through a 20 Å wide region around the 3557 Å peak, with an instrument spectral resolution estimated at about 3 Å. The zero of the θ ordinate is arbitrary and reflects apparatus adjustments. The general vertical displacement between curves C and A, with magnetic field off and on, respectively, is real but consists mostly of background Faraday rotation.

As discussed in Sec. II, a dispersionlike spurious optical rotation is seen in our curves with $H=0$, and such a pattern clearly marks the 3557 Å peak position in curve C of Fig. 3. With $H=12$ kG applied (curve A) we see a large net Faraday rotation $(\theta_A-\theta_C)$ and the net pattern due to the 3557 Å peak is again dispersion-like. (By rotating the incident beam polarization we could actually null out the zero-field rotation or reverse it in sign, relative to the Faraday rotation, as pointed out in II.)

With H set on the F-center ESR resonance ($g=2.0001$), saturating the resonance with microwave power was seen to "quench" the H-dependent rotation pattern of the 3557 Å line completely (to within the noise fluctuations in the trace)—effecting the transition A → B in the figure. The change in mean vertical posi-

tion between A and B represents the change in θ_{para} of the broad F band itself, the broad-band rotation being slowly varying (with λ) across this small spectral increment. Curves B and C are sensibly identical, apart from the vertical displacement; the latter is due to background rotation (Dewar windows, fundamental interband rotation, etc.), which is sensibly λ-independent on this horizontal scale. The rotation of the sharp line is strongly paramagnetic, and no appreciable diamagnetic component is visible.

The resonance character of the sharp-line FR-ESR signal, with respect to the F-center ESR spectrum, is shown in the upper right in Fig. 3. Sweeping H slowly through H_0 (resonance) with moderate microwave power on carries us from curve A to B and back. The resulting trace of $\Delta\theta(H)$ must reflect the ESR absorption line. However, for reasons previously referred to (Sec. II and Ref. 6), we cannot expect to see the intrinsic width and shape due to at least one spurious broadening, a relaxation-time broadening due to the long T_1 ($\sim$20 sec); the width of the observed $\Delta\theta(H)$ peak generally increases with sweep rate and power. To overcome this one must sweep through the ESR line, of width <1 G, in a time long compared to T_1 and with very small microwave power; we do not have sufficiently good system stability to do this. Rapid-passage inversion experiments [as in Fig. 2(a)] were not carried out on the sharp-peak rotation; however, the relaxation time after simple saturation appeared to be the same as for the broad F-band rotation. The width and position (H_0) of the $\Delta\theta(H)$ resonance was the same when observed either on one of the sharp-peak rotation maxima or at any λ in the broad-band pattern to within the effective resonance width of $\sim$10 G.

For quantitative consideration, we show in Fig. 4 the sharp-peak paramagnetic rotation $\theta(\lambda)$, i.e., $\theta_A-\theta_B$ from Fig. 3, together with the absorption $\alpha(\lambda)$. To avoid error in comparison, we evaluated $\alpha(\lambda)$ directly from a recording of the transmitted light $I(\lambda)$ reaching the photomultiplier in the Faraday-rotation apparatus,[6] by plotting $\alpha(\lambda)=t^{-1}\log[I(\lambda)/I_0]$, where t is the sample thickness. The incident intensity I_0 is properly $I_0(\lambda)$, but over the 20 Å span studied is sensibly taken constant. The constant was not direcly measured; thus, the zero of the α ordinate in Fig. 4 is rather arbitrary, but absorption changes, e.g., the zero-phonon peak height, are accurate to within $\pm$10% as read from the scale given.

The 3557 Å peak is evidently not shown with its true width with our available resolution, i.e., when viewed with the minimum monochromator slit width, as noted from the narrowing of the line as the slit is reduced (Fig. 4) from 0.05 to 0.016 mm, corresponding to slightly over 3 and 1 Å resolution, respectively, in this spectral region. The smallest slit setting in our machine (Perkin-Elmer 350 monochromator) is 0.01 mm. But signal-to-noise ratio limitation restricted the slit setting in Faraday-rotation measurement to $\gtrsim$0.03 mm, and in absorption measurement to $\gtrsim$0.015 mm. A subsequent higher-resolution spectrum[14] has shown a typical true width of about 0.5 Å for the zero-phonon line. Thus, our absorption trace with 0.016-mm slit falls short of resolving the line.

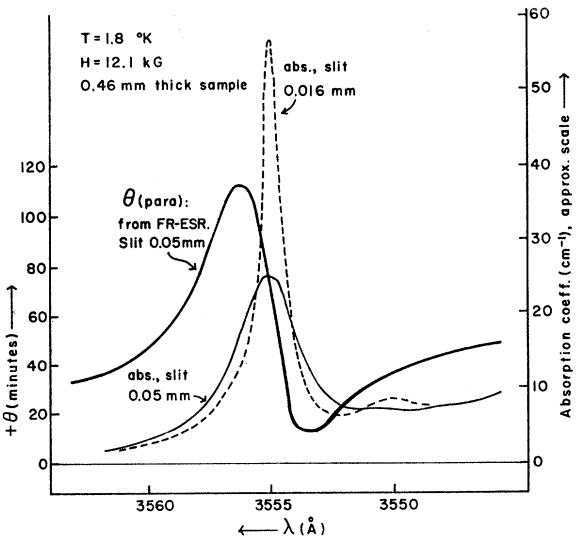

FIG. 4. The 3557 Å line paramagnetic Faraday rotation, taken as the difference $\theta_A-\theta_B$ from Fig. 3. The sample absorption as measured directly in the Faraday-rotation apparatus is also shown, for two monochromator slit settings corresponding to resolutions $\sim$4 and $\sim$1.5 Å. This was computed as in $[I_0/I(\lambda)]$ from the transmitted intensity $I(\lambda)$, with I_0 assumed constant over this narrow λ range. Because a minimum light level was required for reliable rotation signals it was not possible to completely resolve the rotation pattern; therefore to make numerical comparison of the θ and absorption amplitudes one should use the same resolution for each measurement. A nonlinear measurement effect due to simultaneous high absorption and finite resolution must be corrected for as described in the text. Discrepancy between the assigned 3557 Å peak value (Ref. 14) and the one we indicate is probably due to a slight inaccuracy in our wavelength drive.

Traces of $\theta(\lambda)$ were examined with a sequence of slit widths down to about 0.02 mm. At this or smaller slit settings, a noise-rectification effect in the measuring system (electronic phase meter) made the recorded rotation peak amplitudes somewhat untrustworthy. But down to this range at least the pattern increased uniformly in amplitude and decreased in width with decreasing slit width, and remained generally dispersion-like in shape, i.e., of the shape of the dispersion $\phi(\lambda)$ that one would calculate for the observed 3557 Å absorption line.

The paramagnetic character of the rotation of the line, and the close association with the F center, is clearly shown by the double-resonance results. A plot of the H-field dependence of the amplitude of the pattern was also made over the range 0–40 kG at 1.8°K. This showed a simple saturation, following the function $\tanh(g\beta H/kT)$ to within some 10% experimental error, characteristic of an $S=\frac{1}{2}$ system, with $g\simeq 2$. The dia-

[14] W. A. Runciman and A. E. Hughes (private communication).

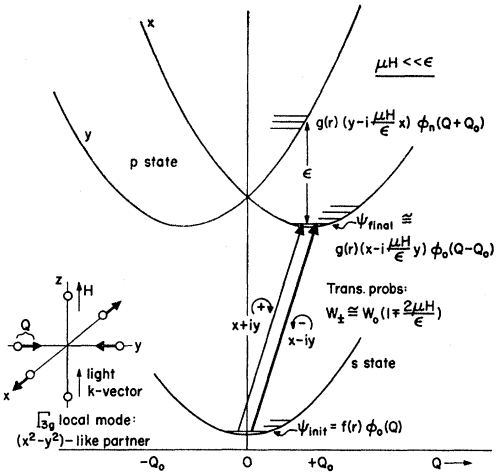

FIG. 5. Simple model for the zero-phonon Faraday rotation, in terms of Jahn-Teller interaction in the F-center p state with a single noncubic mode. The mode exemplified is one partner of the twofold E_g mode, sketched at lower left; the other partner does not split the x-like and y-like states and is not important. The basic mechanism of the magneto-optic coupling is partial unquenching of the orbital momentum by "vertical" mixing between the x and y states by the operator L_z. For simplicity spin is omitted in the sketch, which actually describes the diamagnetic rotation and circular dichroism; the mechanism with spin is essentially the same, with mixing proceeding via spin-orbit coupling $\mathbf{L}\cdot\mathbf{S}\sim L_z S_z$. The limit $n\gg 1$, where n is the number of vibrational quanta in either Jahn-Teller well, is pictured. The model predicts a simple dispersionlike $\theta(\omega)$.

magnetic term, which determines the slope of $\theta(H)$ in the high-H region ($g\beta H\gg kT$), was very small and could not be determined because of the limited accuracy of this type of measurement with our apparatus. The accurate value of g is given by the double resonance; bearing in mind the width in Gauss of the observed resonant interaction $\theta(\Delta H)$ (Fig. 3) we quote $g=2.000\pm 0.002$.

V. DISCUSSION: MAGNETO-OPTIC CHARACTER AND IDENTITY OF 3557 Å LINE

A. Jahn-Teller Model in Semiclassical Limit

The outstanding features of the rotation pattern we see for this line are the dispersion shape and the definite sign ("positive" low-energy peak). Dispersion shape arises when either the initial or final state (or both) of a transition is an orbital singlet, or more generally, is an incomplete orbital manifold,[6] as opposed to transition between two unresolved but complete orbital manifolds (as in the over-all F-band rotation), which gives a dispersion derivativelike pattern. If the 3557 Å line is taken to be the F-center zero-phonon line, the dispersionlike rotation demands that the p state be split by the Jahn-Teller effect, the final state of the transition being one with quenched or partly quenched orbital momentum.

In Fig. 5 is illustrated the basic mechanism which we feel accounts for the shape and sign of the zero-phonon rotation and predicts the right order of magnitude for the amplitude. For simplicity, a spin-free model is sketched. The model is general, but to be specific we envision only the coupling to a particular mode, taken to be the local $\Gamma_{4g}(E_g)$ mode made up of radial displacements of the nearest six cations; it is likely that this is the mode most strongly coupled to the F electron of the even-parity noncubic modes. This mode happens to have the property that it does not couple the electronic states if for the latter we chose the cartesian x-like, y-like, and z-like functions. This allows us to think in terms of purely static Jahn-Teller splitting: In the absence of magnetic or similar perturbations, the eigenstates remain purely x-like, y-like, etc., their being no vibronic mixing as in the more general Jahn-Teller effect.[15] For the light k vector and magnetic field along z, a (100) direction, we need use only the single configuration coordinate Q of that mode (of the two degenerate E modes) that couples the x-like and y-like states; the other mode and the z-like state are not significant. An applied H field now causes a small admixture into the x-like and equivalent y-like states at the bottoms of the two Jahn-Teller potential wells, generating finite angular momenta $\langle L_z\rangle$ which must account for any magneto-optical properties. In the semiclasscial limit in which the Jahn-Teller wells contain many vibrational quanta, the magnetic admixture must proceed only "vertically," i.e., across the gap of energy ϵ between the potential curves at the equilibrium coordinates $\pm Q_0$; "horizontal" admixture is negligible because of the small overlap between the two vibrational functions $\phi_0(Q\pm Q_0)$. Straightforward first-order perturbation (see Fig. 5) gives a magnetic circular dichroism, i.e., fractional difference of transition probabilities for light of left-versus-right circular polarizations, of size $s\equiv(W_+-W_-)/W_0=(4\mu H/\epsilon)$. Since the final states (i.e., those in bottoms of the two wells) are not split nor shifted in first order, but only rendered slightly impure, the spectral shape of the circular dichroism is simply that of the absorption and the Faraday rotation has the shape of the dispersion.

If spin is included, we replace the H-field Zeeman interaction μH of Fig. 5 by the effective spin-orbit energy $\lambda\langle S_z\rangle=(\frac{1}{2}\lambda)\tanh(\mu H/kT)$, assuming the spin-orbit interaction as quenched in first order, i.e. $|\lambda|\ll\epsilon$. This gives

$$s=(2\lambda/\epsilon)\tanh(\mu H/kT) \qquad (4)$$

for the magneto-optic parameter s defined above, to which the magnetic circular dichroism and Faraday rotation are proportional. Specifically, this represents the paramagnetic part which normally dominates at helium temperatures in paramagnetic centers.

[15] See various papers on the dynamical Jahn-Teller effect, such as Frank S. Ham, Phys. Rev. 138, A1727 (1965). Note that when the three-dimensional aspects of the E-mode interaction are correctly incorporated, the factor 2 in the exponent in Eq. (5) is replaced by $\frac{8}{2}$—see Eq. 2.10 of Ham's paper.

For a spectral line we have an absorbance $a(\omega)=t\alpha(\omega)=2t(\omega/c)n_2(\omega)$, and corresponding dispersion $\phi(\omega)=t(\omega/c)n_1(\omega)$, where t is the sample thickness and $n=n_1+in_2$ is that part of the complex refractive index pertaining to the absorbing species. These are related by $\phi(\omega)=\frac{1}{2}\,\mathrm{KK}\{a(\omega)\}$, where KK means Kramers-Kronig inversion. For the simple case of dispersionlike rotation, the rotation is given by

$$\theta(\omega)=(\tfrac{1}{2}s)\phi(\omega)=(\tfrac{1}{4}s)\,\mathrm{KK}\{a(\omega)\}. \tag{5}$$

For a Lorentz line, in particular, the peak-to-peak dispersion just equals the absorbance peak amplitude a_0. Assuming this line shape, for the F-center zero-phonon line we have, in the semiclassical limit just discussed, a peak-to-peak paramagnetic rotation

$$\theta_{pp}=a_0(\lambda/2\epsilon)\tanh(\mu H/kT). \tag{6}$$

From the measured absorption and rotation amplitudes we can estimate ϵ from (6) [since λ is known from (3)]. However, we are dealing with imperfectly resolved $a(\omega)$ and $\theta(\omega)$ (Fig. 4). It seems logical that Eq. (5) should relate not only the intrinsic (resolved) $a(\omega)$ and $\theta(\omega)$, but also those observed using a light beam of given but arbitrary spectral distribution $g(\omega)$, i.e., using a monochromator with slit function $g(\omega)$. Superficially, it would appear that the imperfectly resolved quantities, which can denote $\tilde{a}(\omega)$ and $\tilde{\theta}(\omega)$, are merely the convolutions of the slit function $g(\omega)$ upon $a(\omega)$ and $\theta(\omega)$; and if the latter are related by the Kramers-Kronig relations, e.g., if $\theta(\omega)\propto\phi(\omega)$ for dispersionlike rotation, then (5) should apply to them also since the Kramers-Kronig relations can be shown to be invariant under convolution. Whether this is true must be examined in the context of the measuring process used. In the Appendix we show that our observed $\tilde{a}(\omega)$ and $\tilde{\theta}(\omega)$, as in Fig. 4, are simple convolutions of $a(\omega)$ and $\theta(\omega)$ on $g(\omega)$ only in the limit in which $a(\omega)\ll 1$ for all ω, i.e., when the absorption of the line is negligible. With large absorption information carried by spectral components of the light beam near the line center frequency is lost because of the attenuation factor $\exp[-a(\omega)]$, and the observed $\tilde{a}(\omega)$ and $\tilde{\theta}(\omega)$ are both degenerated, though in different ways. In the particular limit $(\Gamma/\gamma)\gg\sqrt{a_0}\gg 1$, i.e., strong absorbance but extreme instrumental broadening, where Γ and γ are the slit-function width and the intrinsic linewidth, respectively, it can be shown that $\tilde{a}(\omega)$ has simply the shape of $g(\omega)$; and that for the dispersionlike $\theta(\omega)$ the observed $\tilde{\theta}(\omega)$ is shaped like the dispersion Kramers-Kronig conjugate to $g(\omega)$. The relation (5) applies, wherein $a(\omega)$ and $\theta(\omega)$ are replaced by $\tilde{a}(\omega)$ and $\tilde{\theta}(\omega)$, except for a correction factor $f(a_0)$ which depends nonlinearly on a_0 and on the resolved line shape $a(\omega)$:

$$\theta(\omega)\cong f(a_0)(\tfrac{1}{4}s)\,\mathrm{KK}\{a(\omega)\}\propto\mathrm{KK}\{g(\omega)\} \tag{5'}$$
$$(\text{for range } \Gamma/\gamma\gg\sqrt{a_0}\gg 1).$$

For Lorentz and "rectangular" line shapes the $f(a_0)$ are asymptotically $(\frac{1}{4}\pi)^{1/2}a_0^{1/2}$ and a_0^{+1}, respectively. The apparent rotation is relatively more or less enhanced. For Gaussian $a(\omega)$, $f(a_0)\to(\frac{1}{4}\pi)^{1/2}a_0/(\ln a_0)^{1/2}$ for $a_0\to\infty$, numerically closest to the rectangular $f(a_0)$.

If either or both extremes $\Gamma/\gamma\gg\sqrt{a_0}$ or $\sqrt{a_0}\gg 1$ are relaxed, the exact relation between $\tilde{a}(\omega)$ and $\tilde{\theta}(\omega)$ is not simple, but the nonlinear effect of the $\exp[-a(\omega)]$ attenuation then decreases, and (5′) must continue to hold in an approximate way, but with $f(a_0)$ uniformly approaching unity.

Unfortunately, with our apparatus, especially with the double-resonance feature, we could not get reliable rotation curves with higher resolution or less dense samples than as given in Fig. 4. With an intrinsic width[14] of perhaps 0.5 Å, we have $\Gamma/\gamma\sim 10$ for the solid curves ($\sim$5-Å resolution) in Fig. 4. From the dashed absorbance curve ($\sim$1.5-Å resolution) we can extrapolate a resolved a_0 of $\sim 3\times(50\ \mathrm{cm}^{-1})\times(0.05\ \mathrm{cm})\sim 7$, or $\sqrt{a_0}\sim 2.6$. Thus the nonlinear effect should not be neglected. The resolved $a(\omega)$ is presumably between Lorentz and Gaussian; but since the extreme limiting case mentioned above is hardly realized, using correction factor $f(a_0)\sim 2.5$, close to the Lorentz-line value, should give an appropriate estimate.

Using the data for 0.05-mm slit setting in Fig. 4, $\tilde{\theta}_{pp}=0.03$ rad and $\tilde{a}_0=20\ \mathrm{cm}^{-1}\times 0.05\ \mathrm{cm}=1.0$, and approximating the slit function as Lorentz-like, we can estimate ϵ from $\tilde{\theta}_{pp}=f(a_0)\tilde{a}_0(\lambda/2\epsilon)\tanh(\mu H/kT)$ as in (6), wherein $\tanh(\mu H/kT)=0.4$. If $f(a_0)=2.5$ this gives $|\lambda|/\epsilon\simeq 0.06$; or with $\lambda\simeq -60\ \mathrm{cm}^{-1}$ from (3) above, we find $\epsilon\simeq 1000\ \mathrm{cm}^{-1}$.

The estimate $|\lambda|/\epsilon\sim 0.1$ says that the quenched-orbital-momentum model, requiring ideally $|\lambda|/\epsilon\ll 1$, is at least self-consistent with the data. The model therefore explains the basic observed shape of the rotation. The sign of the dispersionlike pattern (positive low-energy peak) is correctly predicted, since λ is negative; this feature is not clear from the equations we have written, but becomes clear if one considers a diagram as in Fig. 5 with spin included, and notes the relative signs of the zero-phonon and F-band rotations in Fig. 1.

B. Jahn-Teller Model with $n\sim 1$

The above model is rigorously based on the semiclassical limit $n\gg 1$, where n equals $(\frac{1}{4}\epsilon)/(\hbar\omega_{nc})$, i.e., the number of noncubic-mode quanta contained in the Jahn-Teller well of depth $\frac{1}{4}\epsilon$ (Fig. 5). We have no accurate way to determine the appropriate value of $\hbar\omega_{nc}$. From the Huang-Rhys factor S we may estimate the weighted average frequency ω_0 of all modes broadening the F band, using, for example, the relation $S=\Delta/(\hbar\omega_0)$ where Δ is the interval between the zero-phonon line and the F-band peak; and S is obtainable from $\exp(-S)$, the ratio between the integrated zero-phonon and F-band absorbances. Measured values of the latter are still a little suspect in CaO because of the familiar uncertainties of the interference of other absorption bands.

Roughly, the integrated peak-to-band intensity ratio is 10^{-3}, meaning $S\sim 6$. With $\Delta\sim 0.17$ eV ~ 1400 cm^{-1} (see Fig. 1), this gives $\hbar\omega_0\sim 200$ cm^{-1}. If $\hbar\omega_{nc}$ is comparable, then the number n describing the Jahn-Teller depth is of order unity, assuming $\frac{1}{4}\epsilon\sim 250$ cm^{-1}. Clearly we do not have the semiclassical limit in the Jahn-Teller model.

Finite overlap between the degenerate set of lowest vibrational functions in the Jahn-Teller wells, e.g., the pair of functions $\phi_0(Q\pm Q_0)$ of Fig. 5, produces an effective orbital degeneracy and leads to magnetic splittings proportional to[15]

$$\langle x|L_z|y\rangle=\int\phi_0(Q-Q_0)\phi_0(Q+Q_0)dQ=e^{-2n}. \quad (7)$$

Here $\langle x|$ and $|y\rangle$ mean the product vibronic functions $\psi_x(\mathbf{r})\phi_0(Q-Q_0)$ and $\psi_y(\mathbf{r})\phi_0(Q+Q_0)$, i.e., x-like and y-like electronic functions times vibrational functions appropriate to the two respective Jahn-Teller wells. As is well known, this gives "reduced" orbital-Zeeman and/or spin-orbit splittings $2\mu H\langle L_z\rangle$ and $\lambda\langle S_z\rangle\langle L_z\rangle$, equal, respectively, to $2\mu H$ and $\lambda\langle S_z\rangle$ times the overlap factor $\exp(-2n)$. Assuming these splittings to be unresolved, they produce magneto-optic effects of what we call the second kind, i.e., dispersion-derivativelike Faraday rotation, as in the F band.[6,7] If $n\sim 0$, angular momentum is effectively unquenched and magneto-optically the zero-phonon transition is entirely of this type. Short of this limit, one has a competition between a dispersionlike rotation term of order $(A/\epsilon)\phi(\omega)$ and a dispersion-derivative term of order $Ae^{-2n}\partial\phi(\omega)/\partial\omega$, where A stands for either μH or $\lambda\tanh(\mu H/kT)$, diamagnetic or paramagnetic contributions, respectively, and $\phi(\omega)$ is the dispersion. In magnitude, $\partial\phi/\partial\omega$ is of order $|\phi|/\gamma$, where γ is the linewidth. When the rotation pattern is instrumentally broadened, such as through use of a light beam of spectral width Γ, the observed magnitude is rather $|\phi|/\Gamma$. In this case the magnitude of the dispersion-derivative rotation relative to the dispersionlike rotation is of order $e^{-2n}(\epsilon/\Gamma)$.

In our situation, with a resolution of 5 Å or $\Gamma\sim 60$ cm^{-1}, as in the 0.05-mm-slit trace of Fig. 4, and with $\epsilon\sim 1000$ cm^{-1}, the ratio of $(\partial\phi/\partial\omega)$-like to ϕ-like rotations is less than unity if $n>1$. In other words, even in the semiquantum case $n\sim 1$, it is still possible that we observe an approximately dispersionlike pattern. It should be added that the nonlinear measuring effect arising when $\Gamma/\gamma\gg 1$ and $a_0\gg 1$, discussed earlier, would probably further enhance the dispersion character, since the $\partial\phi/\partial\omega$ rotation is more strongly peaked at the center frequency and is thus more subject to the attenuating effect.

In discussing Jahn-Teller splitting in the F center we have implicitly neglected the effect of dynamic (vibronic) coupling.[15] The lattice mode of symmetry E chosen for illustration in the model has zero dynamic coupling via the electron-lattice interaction, as we stressed at the beginning, and the only coupling between the two degenerate modes and between the electronic states is by magnetic or spin-orbit interaction or applied stress. With other modes, namely T modes, there is dynamic coupling. Our understanding is that such coupling should not greatly modify the basic magneto-optical properties of the states, since there is still a certain degree of effective orbital degeneracy governed by the parameter n; if $n\sim 1$, we still expect a magnetic coupling mechanism of the first kind ("vertical" mixing as in Fig. 5) to be operative, since vibronic mixing cannot fully restore effective orbital degeneracy. The principal effect of the mixing is to produce an apparent splitting of the entire absorption band. But this would only be visible if the breadth of the band were largely due to noncubic modes, which does not seem to be true in our case as judged from the fact that our estimated ($\frac{1}{4}\epsilon$), the Jahn-Teller depth, is much less than the F-band width. In any event the F band shows no sign of such splitting.

C. Other Aspects of the Zero-Phonon Line and the CaO F Center

The implication of our results is that the 3557 Å line, the 3.65-eV band, and the familiar $g=2.000$ spin resonance all belong to the same point defect, which we take to be the F center. Some other types of measurements have recently been made which also bear on this assignment. Runciman and Hughes[14] have studied the 3557 Å line under applied uniaxial stress, as well as under strong magnetic fields. The stress-splitting pattern they report is compatible with a defect of cubic symmetry, such as the F center. But they make certain deductions as to the magnitudes of Jahn-Teller and spin-orbit splittings from their data which seem to disagree with those which we estimate. Unfortunately, a direct comparison of their results with ours must wait until their work is published.

Multiphononlike structure is present on the low-energy side of the 3.65-eV band. The most prominent peaks, visible in Fig. 1, are at distances 220 and 325 cm^{-1}, respectively, from the zero-phonon line; there are also at least one or two somewhat less discernable peaks further up on the band. We did not obtain resolved Faraday rotation curves for these peaks. As yet, no definite numerical relationship has been shown between the peak intervals and other data such as the phonon spectrum. However, we may conjecture that if the peaks at 220- and 325-cm^{-1} separation are one-phonon peaks involving the most important vibrational modes, the mean vibrational frequency should be intermediate between these, e.g., the mean value 270 cm^{-1}. With a distance $\Delta\simeq 1300$ cm^{-1} from the 3557 Å line to the band maximum, this implies $S\simeq 5$ for the Huang-Rhys factor (as noted in Sec. V B) a value $S\simeq 6$ is estimated from the ratio of the integrated absorbances of the band and zero-phonon peak.

A good test for identifying the phonon structure with the band is had in the fluorescence spectrum. An emission spectrum obtained from excitation in the 3.65-eV band has been seen by Henderson and King,[16] and independently in our laboratory.[17] We see in fact an emission band which is fairly accurately a mirror image of the absorption band, with respect to reflection through the 3557 Å line; furthermore, the zero-phonon line, and at least the two strongest multiphonon peaks, are present in emission, in harmony with the usual fluorescence model. The S value obtained from the integrated intensity ratio in emission is about 4.5.

Several quantitative predictions of the general F-center model can be applied to the 3.65-eV band. The band half-width at $T=0°$K is given by $W(0)=S^{1/2}(8\ln 2)^{1/2}(\hbar\omega)$, where ω is the mean broadening frequency. For $\hbar\omega=270$ cm^{-1} and $S=5$, this gives $W=1400$ cm$^{-1}=0.18$ eV. This is substantially less than the half-width we see in our samples at $T=4°$K, which is some 0.25 eV. But the observed width is almost surely contaminated by effects from overlapping bands. For example, besides the F center, at least one other irradiation-induced point defect, the F_t center,[18] is known to absorb in this region, as do probably other centers of the F aggregate and other types. In additively colored CaO, the F' band is seen to overlap with the F band. The apparent band shape and width in neutron-irradiated samples depend somewhat on irradiation dosage, and are affected by heat-treating the sample after irradiation. We find that heating, at temperatures short of the F-center annealing point (about 550°C), appears to reduce the density of other species, the F band becoming more well defined and appearing more Gaussian in shape.[5]

Since the F center in oxide crystals is charged, there is an important question about the degree to which the center can be spatially isolated in the lattice. As required for bulk electrical neutrality, the added presence of one or more types of negatively charged bodies must be assumed. These can be in principle interstitial O^- or cation vacancies, in neutron-irradiated crystals, or also charged impurities. The charge compensators may be either randomly distributed, as perhaps in samples neutron irradiated at low to moderate temperatures, or they may be more or less spatially correlated. Direct nearest-neighbor association with such a species, as in the formation of F_2 centers,[11,19] would so modify the F center that we would not identify it as such. The effect of a somewhat more loosely associated charged body, several interionic spacings away, should be a perceptible axial splitting, of both the ground-state g tensor and the zero-phonon line. Taking account of semicontinuous radial and angular distribution, this would show up as unresolved line broadening. Since charge-compensator association must be a downhill (exothermic) process, we should expect evidence of it in samples that have been subject to temperatures permitting some ionic diffusion.

There is a curious effect sometimes present in the ESR spectrum of the CaO F center, described in our earlier paper,[6] which in fact suggests the presence of a nearby, but not nearest-neighbor associated, perturbing species. This is seen clearly in neutron-irradiated samples that have been subjected to a certain heat treatment. We note first that mild heating, at temperatures short of the general F-center annealing point, results in a narrowing of the wings of the F-center line and the destruction of nearby weak lines attributed to aggregate centers; the line becomes well isolated and fairly symmetric, with width about 0.10 G. But further heating, to approximately the F-center annealing point, for such a time that the F-center density is markedly reduced (e.g., by a factor three), causes a very small, imperfectly resolved splitting in the line. The splitting we measure (at X band) is about 0.05 G. There was preliminary indication that the line structure is asymmetric, with the high-H (lower-g) derivative peak being sharper and stronger[20]; this detail seemed not to be entirely reproducible, and spectra of other samples show a sensibly symmetric splitting. A high-resolution study of the line at 35 or 70 GHz would be desirable, but cannot yet be reported. Somewhat analogous structure has been noticed in the F-center line in heated samples of neutron-irradiated MgO,[21] with slight differences; it is premature to suppose that the cause is the same as in CaO.

More than one interpretation of this curious splitting comes to mind. We believe the cause is electrostatic polarization of the F center by a nearby charge, which introduces a small axial difference $g_\perp - g_\parallel$ into the g tensor. The observed line shape is isotropic, thus we must have a continuous or semicontinuous angular distribution of the axes, the derivative spectrum showing peaks of alternate sign at the $g_\perp$ and $g_\parallel$ points, respectively. This is like the familiar spectrum of axial molecules in solution. But here one must also allow for a distribution in the magnitude, as well as the orientation, of the splitting; the actual line shape and asymmetry must depend on the radial distribution of perturbing charges, and might vary with sample treatment. An estimate of the splitting, considering only a mixing of the F-center s and p states by the coulomb field of a point charge, gives $g_\perp - g_\parallel \simeq -(2\lambda/E)n^{-4}$, where E is the F-band energy (of order e^2/a_0 where a_0 is the interionic spacing), λ is the p-state spin-orbit parameter, and the distance to the charge is na_0. This accounts for the measured splitting with a mean value $n\sim 4$, which is consistent with the isotropy of the pattern.

[16] Brian Henderson and R. D. King (unpublished).
[17] Burce D. Evans (unpublished).
[18] D. H. Tanimoto, W. M. Ziniker, and J. C. Kemp, Phys. Rev. Letters 14, 645 (1965).
[19] R. D. King and B. Henderson, Proc. Brit. Cer. Soc. 9, 63 (1967).
[20] Note Fig. 7 of Ref. 6. The caption for that figure has an error—it should read "increasing H ($g<2$) to the right."
[21] W. A. Weeks, also B. Henderson (private communications).

One asks whether this splitting is an intrinsic characteristic of the CaO F center, being simply invisible in nonannealed samples because of miscellaneous line broadening; or whether it arises from the heat treatment. A close look at the line shape and width as a function of heating indicates that (contrary to our earlier opinion[6]) the latter is the case; the net linewidth does not change appreciably from the condition after mild heating to the point where the splitting is seen. The principal broadening of the ESR line, accounting for the width before heat treatment, is probably due to spin-spin interaction. For given distance between species this is much stronger than broadening from the electrostatic-polarization mechanism. Thus there is no necessary connection between the slight linewidth change (reduction of the wings), seen upon mild heating, and the splitting effect.

Of species that qualify as appropriate nearby charge compensators in the case observed, we reject all paramagnetic species, since magnetic spin-spin broadening due to spins as close as $4a_0$ would be several gauss, many times the linewidth. The first choice is cation vacancies. Association of these with oxygen vacancies is one of the two annealing mechanisms for the F center in MgO and CaO.[22] One postulates that an interrupted annealing state is seen in our moderately heated samples, in which those remaining F centers that have not been annihilated to form cation-anion divacancies tend to have nearby cation vacancies, which have approached them under the electric stress. That the cation vacancies can be diamagnetic, as required, is explained by supposing that they have no trapped holes (bare vacancies); though an isolated cation vacancy may carry one or two trapped holes, when the vacancy is near a positively charged F center it is plausible that even one hole is not stably bound. (The implication is that the binding energy of a hole on a cation vacancy is less than that of an electron on an O^{2-} vacancy.)

In this connection we must clarify the status of the F_2 center, i.e., a cation-anion divacancy with one trapped electron, in CaO. This is crucial since confusion with this center would inject ambiguity into our identification of the F-center optical absorption through the magneto-optical double-resonance experiments. The F_2 center was first proposed experimentally to account for an asymmetric ESR line on the high-H ($g<2$) side of the F-center line, seen in neutron-irradiated samples of several IIA oxide compounds.[11] These observations pertained only to powder samples, except in MgO; in single-crystal MgO, the spectrum is known to have the presumed [100]-type symmetry.[19] Heating irradiated MgO converts most or all of the F centers into F_2 centers, which conforms with the cation-anion aggregation process postulated above. In our neutron-irradiated CaO, we see a structured line, of maximum intensity around a tenth that of the F center, lying about 1.0 G to the high-H side of the F center, at the position mentioned in powder samples,[11] i.e., $g(\text{average})=1.9995$. Mild heating removes this line; it does not reappear under further heating, as the F center begins to anneal out. The characteristic shape of the F-center line during advanced annealing, with the splitting, is somewhat reminiscent of the F_2 line shape. But this is superficial: For one thing there is no shift of the F-center line from its position before heating ($g=2.0001$); and in view of the 0.10-G F-center linewidth, the F_2 spectrum would be well resolved from it. Secondly, the F_2 spectrum must be clearly anisotropic, which the structured F-center line is not. We suspect that cation-anion vacancy association arises as freely in CaO as in MgO, but that the binding energy of an electron in the divacancy is sufficiently less in CaO so that the F_2 electron is only marginally trapped; a slight shift in the crystal Fermi level, as would result from heating or other treatment, could result in all divacancies being void of electrons in electronic thermal equilibrium.

Another point defect that could qualify as the charge compensator for the F center is a hydrogen species, e.g., H^+ in a substitutional Ca^{2+} site. Some hydrogen is understandably present in CaO as hydroxide. In this case the heat-induced splitting of the ESR line could be merely a hyperfine splitting. Crude estimates would place the mean proton distance at some $3a_0$, to account for the splitting, from either contact or dipole-dipole terms. But it is interesting that at this distance the splitting due to the electrostatic-polarization mechanism would seem of the same order of magnitude. As with any other postulated species, direct (nearest neighbor) association would destroy the F center in its observed form.

Charge-compensator association has obvious implications for the optical spectrum, at least for the zero-phonon line, and the magneto-optic properties. If one considers only polarization mixing of the $1s$-like and $2p$-like states, there is a simple proportionality between the g-tensor splitting and the splitting ΔE of the $2p$ state, namely $\delta g=g_\perp-g_\parallel\simeq-(2\lambda/E)(\Delta E/E)$. The detected $|\delta g|\sim3\times10^{-5}$ then implies $\Delta E\sim150$ cm^{-1}. This would be manifested as a resolved multiplicity of the zero-phonon line, if the magnitude of δg were dis-

[22] The other is recombination of interstitial oxygen with O vacancies. Since interstitial O would most likely exist as O^- or conceivably atomic oxygen, both of which are paramagnetic, we are led to reject such oxygen as the nearby species producing the effect as observed. It has been speculated that interstitial cations and anions, though produced in comparable numbers with vacancies by knock-on neutron collisions, may somehow spontaneously recombine with each other during irradiation (at least for irradiations at $T\gtrsim300$°K), forming "positive" dislocation loops; what remains are only the vacancies. At any rate no experimental detection of either interstitial oxygen or cations has ever been reported in the IIA oxides, though there are unidentified optical bands which could be related to such species. Yet there is also a problem with the supposition that cation vacancies are present in our neutron-irradiated samples, namely the lack of a detectable number of V_1 centers (one trapped hole) as seen by ESR; this could be a matter of the crystal Fermi level, i.e., it might be that holes are not stably trapped at cation vacancies when anion vacancies are also present.

crete, as with close-in charges; the stress-splitting patterns of the component lines would have definite anisotropy. If δg had an almost continuous distribution, roughly true if the mean distance were $\sim 4a_0$, the line would be broadened, to a width ~ 20 Å.

The sample used in the Faraday-rotation experiments of the present paper was one that had been heat-treated only to the first stage, suppressing the aggregate-center optical bands and the weak ESR lines near the F-center line. No splitting was detectable in the ESR line. If, as suggested by the ESR studies with our interpretation, the F centers are spatially well isolated before the onset of charge-compensator association, the Faraday-rotation and stress-splitting patterns of the zero-phonon line in such samples should be those of a cubically symmetric center (apart from Jahn-Teller effects). Generally we see the zero-phonon line in nonheated neutron-irradiated samples, with F-center densities in the range 10^{17}–10^{18}/cm^3, and it persists after mild heating with no very noticeable change in appearance.[7] But no systematic investigation of the effect of annealing on the zero-phonon line, through the point of onset of the ESR splitting, has yet been done; and the conjectured splitting or broadening of the line has not been observed. Studies of the F band, made without attention to the sharp-line structure, showed that no radical change such as a shift or splitting occurs in the band over the entire course of annealing out of the F centers, apart from the loss of the neighboring bands and a slight narrowing.[5] The above-suggested electrostatic splittings of the order 100 cm^{-1} would of course not be expected to much perturb the broad-band shape, nor its associated Faraday-rotation curve.

Additively colored CaO crystals[23] show the same 3.65-eV band and 3557 Å zero-phonon line, and the familiar F-center ESR line, in the same intensity ratios as in neutron-irradiated CaO. We have not examined the Faraday rotation in these crystals. The ESR line has the same width as in slightly annealed neutron-irradiated samples and shows no structure, in the few samples available for study.

ACKNOWLEDGMENTS

Very useful correspondence with Dr. W. A. Runciman, Dr. A. E. Hughes, and Brian Henderson on aspects of this paper is gratefully acknowledged. Important portions of this work are described in the doctoral thesis of one of us (W. M. Z., Ref. 7).

APPENDIX: UNRESOLVED ABSORPTION AND OPTICAL ROTATION MEASUREMENTS

If a light beam of incident strength I_0 with a normalized spectral distribution $g(\omega)$ is passed through a sample of absorbance $a(\omega)$,[24] the transmitted intensity is

$$I(\omega)=I_0\int g(\omega-\omega')e^{-a(\omega')}d\omega', \tag{A1}$$

and one measures an apparent absorbance defined by

$$\tilde{a}(\omega)\equiv\ln[I_0/I(\omega)]. \tag{A2}$$

If an optical rotation $\theta(\omega)$ occurs in the sample, in the transmitted beam we will in fact measure a weighted average rotation:

$$\tilde{\theta}(\omega)=\arg\{\int g(\omega-\omega')e^{-a(\omega')}e^{i\theta(\omega')}d\omega'\}. \tag{A3}$$

In the limit $a(\omega)\ll 1$ for all ω, which normally implies also $|\theta(\omega)|\ll 1$ also, we can expand the exponentials and reduce these expressions to

$$I(\omega)/I_0\cong 1-\int g(\omega-\omega')a(\omega')d\omega', \tag{A1'}$$

and further,

$$\tilde{a}(\omega)\cong\int g(\omega-\omega')a(\omega')d\omega'; \tag{A2'}$$

and similarly in (A3), using $\exp[-a(\omega)]\cong 1$,

$$\tilde{\theta}(\omega)\cong\int g(\omega-\omega')\theta(\omega')d\omega'. \tag{A3'}$$

In this linear limit $\tilde{a}$ and $\tilde{\theta}$ are just convolutions of a and θ on $g(\omega)$. If specifically $\theta(\omega)\propto\phi(\omega)$ where ϕ is the dispersion conjugate to $a(\omega)$, it is then easy to show that $\tilde{\theta}(\omega)$ is similarly proportional to the dispersion Kramers-Kronig-conjugate to $\tilde{a}(\omega)$, so we write $\tilde{\theta}(\omega)\propto \mathrm{KK}\{\tilde{a}(\omega)\}$.

For finite $a(\omega)$ the integrations in (A2) and (A3) are hardly trivial. In Faraday rotation and sometimes in other types of optical rotation, even with appreciable $a(\omega)$ it is often true that $|\theta(\omega)|\ll 1$ for all ω, so that $e^{i\theta}\cong 1+i\theta$ in (A3), which simplifies to:

$$\tilde{\theta}(\omega)\cong[I_0/I(\omega)]\int g(\omega-\omega')e^{-a(\omega')}\theta(\omega')d\omega'. \tag{A4}$$

Of special interest is the situation

$$\Gamma/\gamma\gg\sqrt{a_0}\gg 1,$$

where Γ and γ are the half-widths of $g(\omega)$ and the absorption line, respectively, and a_0 is the peak amplitude of $a(\omega)$. Large a_0 means that within a width γ the sample is opaque; the only information on absorption and rotation in the transmitted beam is carried by spectral components on the far wings of the line. The condition

[23] J. C. Kemp, W. M. Ziniker, and E. B. Hensley, Phys. Letters **25A**, 43 (1976).

[24] There is an analogous nonlinear broadening and distortion of spectral lines which is familiar in astrophysics, under the curious heading "growth curves"; we refer to *Astrophysics*, edited by J. A. Hynek (McGraw-Hill Book Co., New York, 1951), p. 54. The effect on dispersion (and rotation) measurements under high-absorbance conditions is not considered in that connection.

$\Gamma/\gamma \gg \sqrt{a_0}$ means the sample is transparent over most of $g(\omega)$, so that $I(\omega)=I_0-\epsilon(\omega)$, where $\epsilon \ll I_0$; and $g(\omega)$ can be effectively taken outside the integral in (A1), as follows: If we write

$$e^{-a(\omega)}=1-[1-e^{-a(\omega)}]$$

and use the fact that $1-e^{-a(\omega)}$ is sharply peaked within a width $\gamma\sqrt{a_0}$, (A2) and (A3) become

$$I(\omega)=I_0\left\{1-\int g(\omega-\omega')[1-e^{-a(\omega')}]d\omega'\right\},$$

$$\tilde{a}(\omega)\cong\int g(\omega-\omega')[1-e^{-a(\omega')}]d\omega'\cong g(\omega)\times\int[1-e^{-a(\omega')}]d\omega'. \quad \text{(A5)}$$

Now using $I(\omega)\equiv I_0$ we can write (d) as

$$\tilde{\theta}(\omega)\cong\int g(\omega-\omega')\theta(\omega')d\omega'-\int g(\omega-\omega')[1-e^{-a(\omega')}]\theta(\omega')d\omega'. \quad \text{(A6)}$$

Consider dispersionlike rotation, $\theta(\omega)\propto\phi(\omega)$. In the far wings of the line, for fractionally narrow lines[13] the dispersion is approximately $\phi(\omega)=(\pi\omega)^{-1}\int a(\omega')d\omega'$, so that $\theta(\omega)\propto(1/\omega)$. Also in the far wings, $1-e^{-a(\omega)}\cong a(\omega)$; if $a(\omega)$ falls off at least as fast as $1/\omega^2$ the second integral in (f) is at most of order $\sqrt{a_0}/(\Gamma/\gamma)$ relative to the first and is therefore negligible. In the first integral, for $\Gamma/\gamma\gg 1$ the major contribution comes from the far wings, in which we can write $\theta(\omega)=(\frac{1}{4}s)(1/\pi\omega)\times\int a(\omega')d\omega'$, where s is a constant. Using this and upon changing variables $\omega-\omega'\rightarrow\omega'$, the first integral in (A6) gives

$$\tilde{\theta}(\omega)\cong(\tfrac{1}{4}s)\int a(\omega')d\omega'\times\frac{1}{\pi}\int\frac{g(\omega')d\omega'}{\omega-\omega'}. \quad \text{(A7)}$$

The integral over $g(\omega)$ is just the Kramers-Kronig dispersion of $g(\omega)$, in the narrow-line approximation.[13] Comparing (A5) and (A7), we see

$$\tilde{\theta}(\omega)=(\tfrac{1}{4}s)f(a_0)\ \mathrm{KK}\{\tilde{a}(\omega)\}, \quad \text{(A8)}$$

where

$$f(a_0)=\int a(\omega)d\omega\Big/\int[1-e^{-a(\omega)}]d\omega.$$

For $a(\omega)\ll 1$ this $f(a_0)\rightarrow 1$ as it should, agreeing with (A2′) and (A3′). Relation (A8) is just (5′) of the text.

For a rectangular line, $a(\omega)=a_0$ for $|\omega|<\frac{1}{2}\gamma$ and $a(\omega)=0$ elsewhere, it is easily seen that $f(a_0)=a_0$. For a Lorentz line, $a(\omega)=a_0/[1+(\omega/\gamma)^2]$, as $a_0\rightarrow\infty$ we can show that asymptotically $f(a_0)=(\frac{1}{4}\pi a_0)^{1/2}$; for a Gaussian $a(\omega)=a_0\exp[-\frac{1}{2}(\omega/\gamma)^2]$, $f(a_0)\simeq(\frac{1}{4}\pi)^{1/2}a_0/(\ln a_0)^{1/2}$ as $a_0\rightarrow\infty$.